Thermoreversible Behavior of Associating Polymer Solutions: Thermothinning versus Thermothickening

Dominique Hourdet,*,† Jayant Gadgil,† Klara Podhajecka,† Manohar V. Badiger,‡ Annie Brûlet,§ and Prakash P. Wadgaonkar‡

Physico-chimie des Polymères et des Milieux Dispersés, UMR 7615, UPMC-CNRS-ESPCI, 10 rue Vauquelin, 75005 Paris, France; Polymer Science and Engineering Division, National Chemical Laboratory, Pune, India; and Laboratoire Léon Brillouin (UMR 12), CEA Saclay, 91191 Gif-sur-Yvette Cedex, France

Received April 13, 2005; Revised Manuscript Received June 8, 2005

ABSTRACT: Self-assembling properties of poly(sodium acrylate) grafted with dodecyl [C12], PAAgC12, or poly(*N*-isopropylacrylamide) [PNIPA] side chains, PAAgPNIPA, were studied in unentangled semidilute aqueous solution. While PAAgC12 self-associates through hydrophobic interactions, the gelation of PAAgPNIPA is triggered by heating in response to the lower critical solution temperature of PNIPA (LCST ∼ 32 °C). The local structure of the physical networks was investigated by small-angle neutron scattering, and the scattering patterns were described using a polydisperse sphere model taking into account hard-sphere interactions. This model allow us to draw a realistic picture of physical gels with quantitative information concerning the size of hydrophobic cores, the volume fraction of stickers in the aggregates, the fraction of stickers which take part in the aggregation process, the range of repulsive interactions, and the structural modifications induced by temperature. The description of the network is in good agreement with complementary data obtained from DSC and ^{13}C NMR. In the present work, a special emphasis has been given to the important relationship existing between the viscoelastic properties of associating polymer solutions and the binding energy of stickers leaving temporarily the micellar junction. Depending on the endothermic or exothermic nature of the disengagement process of the sticker (heat of demicellization), the relaxation time of the network and the viscoelastic properties will either decrease or increase with the temperature. The consequence is that aqueous solutions of PAAgC12 and PAAgPNIPA exhibit opposite rheological properties with the temperature, namely thermothinning and thermothickening. By mixing these two copolymers, we show that intermediate properties can be obtained but in that case a microphase-separated network is obtained as a result of copolymer segregation.

Introduction

Because of the ever-increasing development of water-based formulations, for both environmental and economic reasons, associating water-soluble polymers have received a lot of attention in the past two decades.[1−5] These amphiphilic macromolecules contain (1) a hydrophilic part (neutral or ionic) that maintains the solubility of the polymer in water and (2) a hydrophobic component (alkyl, perfluoroalkyl, aromatic) which provide the associative behavior. In water, these polymers self-assemble to form hydrophobic clusters, which are embedded in a sea of hydrophilic chains. In semidilute solution the dynamic properties of these physical networks are closely related (1) to the degree of overlapping or entanglement of macromolecular chains and (2) to the properties of the stickers.[6−11] In the case of hydrophobically modified water-soluble polymers, it has been experimentally shown that the characteristic time of the network increases with the strength of the associations: typically the size of the alkyl chain or the fluorine/hydrogen ratio in perfluoroalkyl chains.[6−8] Actually, most of theoretical works on associating polymers[12−15] point out that the characteristic time of the network (τ_N) is proportional to the lifetime of the sticker in the micellar junction (τ_b). This can be expressed by the equation

$$\tau_N \sim \tau_b = \tau_0 \exp(W/kT) \quad (1)$$

where τ_0 is a microscopic time corresponding to the sticker diffusion ($\tau_0 \sim 10^{-9}$ s)[13] and W the potential barrier which depends both on the binding energy and on the additional activation barrier.

From this relation, one can easily understand that the dynamics of the network will slow down either by increasing the hydrophobicity of the sticker (binding energy) or by decreasing the temperature. This is the general feature of aqueous or organic amphiphilic polymer solutions subjected to temperature changes; the relaxation time and the viscosity decrease when the temperature increases. The higher the binding energy, the higher will be the viscosity drop with increasing temperature.

Of course, there are a number of applications where aqueous-based fluids are subjected to heating and cooling cycles, like cooking processes in the food industry, drilling fluids or well cementing operations in deep subterranean formations, paper manufacturing, etc. A technological solution for specific applications where a high viscosity is needed at high temperature can be provided by thermothickening polymers, which are able to self-associate above certain critical conditions. This phenomenon, opposite to the most common feature of gelation upon cooling, was initially reported with cellulosic derivatives.[16−18] It is only during the past 15

† UMR 7615, UPMC−CNRS-ESPCI.
‡ National Chemical Laboratory.
§ Laboratoire Léon Brillouin (UMR 12).
* To whom correspondence should be addressed: Tel +33 (0)1 40 79 46 43; Fax +33 (0)1 40 79 46 40; e-mail dominique.hourdet@espci.fr.

10.1021/ma050786r CCC: $30.25
Published on Web 08/30/2005

years that this specific property has been described for synthetic block copolymers[19−21] and clearly exemplified with graft copolymers[22−27] tailored with responsive side chains, i.e., polymer chains characterized by a lower critical solution temperature (LCST) in water.

Thermothinning and thermothickening associating systems generally exhibit opposite properties and have been dealt with separately in the past. The primary objective of the present study was to bridge the gap between these thickeners and to take benefit of their antagonistic behaviors for a better control of the rheological properties. We wish to report two different approaches taking into account (1) the possibility of mixing different polymers having different stickers (study of mixtures between thermothinning and thermothickening polymers) or (2) the possibility of incorporating different stickers into the same polymer backbone (study of double-grafted copolymers). The purpose of the present paper is to study the rheological behavior of these systems in semidilute solutions and to give a general description of aqueous solutions of thermothinning and thermothickening polymers separately or as a mixture of these two in terms of control of self-assembling, structure, and viscoelastic properties.

Experimental Part

Materials. *N*-Isopropylacrylamide [NIPA] and dodecylamine [C12] were purchased from Aldrich and were used without further purification. Potassium persulfate (Prolabo), 2-aminoethanethiol hydrochloride (Fluka), dicyclohexylcarbodiimide (DCCI; from Acros Organics), and *N*-methylpyrrolidone (NMP; from SDS) were all analytical grade reagents. Water was purified with a Millipore system combining inverse osmosis membrane (Milli RO) and ion-exchange resins (Milli Q). The syntheses of precursors and modified copolymers can be summarized briefly as follows:

Copolymer Precursors. Poly(acrylic acid) [PAA] was obtained as 35 wt % solution in water from Aldrich. The solution was diluted and purified by ultrafiltration (30 000D membrane cutoff) prior to freeze-drying. The number-average molecular weight and polydispersity index determined by size exclusion chromatography (SEC) on neutralized PAA under sodium salt form were $M_n = 50\ 000$ g/mol ($\bar{x}_n = 530$) and $I_p = 3.5$, respectively.

Amino-terminated poly(*N*-isopropylacrylamide) [amino-PNIPA] was prepared by telomerisation of NIPA in water using 2-aminoethanethiol hydrochloride as chain transfer reagent and redox initiator coupled with potassium persulfate.[28] In a three-necked flask equipped with a reflux condenser, a magnetic stirrer, and nitrogen feed, 10 g of NIPA (90 mmol) was dissolved in 100 mL of water, and the solution was deoxygenated for 1 h with nitrogen bubbling. The initiators KPS (0.9 mmol) and AET,HCl (1.8 mmol) were separately dissolved in 10 mL of water prior to be added to the NIPA solution. The reaction was allowed to proceed at a controlled temperature of 20 °C. After 4 h, an appropriate amount of sodium hydroxide was added to neutralize the hydrochloride ions, and the polymer was recovered by dialysis against pure water (membrane cutoff = 6000−8000 Da) and freeze-drying. The amino-PNIPA samples were characterized by ^{1}H NMR spectroscopy, potentiometric titration, and SEC. A number-average molecular weight of 6000 g/mol and a polydispersity index around 2 were obtained.

Grafting of Amino-Terminated Precursors onto PAA. In a three-necked flask, equipped with a reflux condenser and a magnetic stirrer, PAA was dissolved in NMP for 18 h at 60 °C using a thermoregulated oil bath. Amino-terminated chains (C12 or PNIPA) and DCCI were separately dissolved in NMP at the same temperature. The solution of C12 (or PNIPA) was then introduced slowly into the reaction mixture followed by a dropwise addition of DCCI solution. After 20 h, the flask was immersed in a cold water bath, and the insoluble byproduct dicyclohexylurea was filtered off. The copolymer was then precipitated by dropwise addition of a concentrated NaOH aqueous solution. It was recovered by filtration and washed several times with methanol prior to drying under vacuum overnight at room temperature. The copolymer, under powder form, was dissolved in water ($C_p \sim 5$ wt %), centrifuged in order to eliminate the remaining insoluble dicyclohexylurea, and finally purified by dialysis for a period of 1 week against pure water (with membranes of MWCO of 6000−8000 Da) and freeze-dried.

Table 1. Nomenclature and Composition of Grafted Copolymers

copolymers	grafting ratio (mol %)[a] PNIPA	grafting ratio (mol %)[a] C12	grafting yield (%)	M_{eq} (g/mol)[b]
PAA				94
PAAg5C12		5	100	101
PAAg10C12		10	100	108
PAAgPNIPA	0.4		35	120

[a] Number of side chains per 100 acrylic acid units. [b] Average molar mass per monomer unit of the main chain (PAA under Na salt form).

The average composition of copolymers, obtained from ^{1}H NMR, is reported in Table 1.

Preparation of the Solutions. Aqueous polymer solutions were prepared by gentle mixing during a minimum of 24 h before analysis. To compare the solution properties of grafted copolymers having very different weight fraction of side chains, we will refer to the molar concentration of acrylic units belonging to the backbone per kg of solution (in mol/kg):

$$m_A = C/M_{eq} \tag{2}$$

with C, the copolymer concentration (in g of copolymer per kg of solution), and M_{eq}, the average molar mass per monomer unit of the backbone in g/mol (see Table 1).

Rheology. Viscoelastic properties of copolymer solutions ($m_A = 0.3-0.6$ mol/kg) were studied in the linear regime with a strain-controlled rheometer (Rheometrics RFS2), using a Couette geometry. The samples were covered by a thin layer of oil in order to avoid evaporation of water during the measurements. No influence of oil on the rheological behavior of the samples was observed, and the reproducibility was verified for all the experiments. Complementary studies were also performed with a stress-controlled rheometer (Haake RS150) equipped with a cone/plate geometry. After preliminary frequency scans, recorded at different temperatures, the linear regime was identified and the experimental conditions were fixed at constant frequency and shear stress 1 Hz and 5 Pa, respectively. The storage and elastic moduli as well as complex viscosity were recorded during temperature ramping with heating and cooling rate of 2 °C/min.

Differential Scanning Calorimetry. Responsive properties involving PNIPA phase transition were studied by differential scanning calorimetry (DSC) with a microDSCIII from Setaram. Polymer solutions ($V \cong 0.8$ mL), equilibrated with a reference filled with the same quantity of solvent, were subjected to temperature cycles between 10 and 70 °C with a heating and cooling rates of 1 °C/min. These conditions were used to work under thermodynamic control and to avoid any kinetic interference.

Small-Angle Neutron Scattering (SANS). SANS experiments were performed at Laboratoire Léon Brillouin, Saclay (France). Two sets of experiments were carried out using an incident neutron beam of wavelength $\lambda = 5$ and 12 Å with a corresponding sample-to-detector distance of 1.7 and 4.6 m, respectively. These configurations provide a scattering vector modulus [$q = (4\pi/\lambda)\sin(\theta/2)$] ranging between 0.003 and 0.24 Å^{-1} (θ is the scattering angle). Samples were dissolved in D_2O at room temperature and transferred into 5 mm thick quartz containers for SANS experiments. To obtain the coherent scattering intensity of the copolymer, the signal given by the

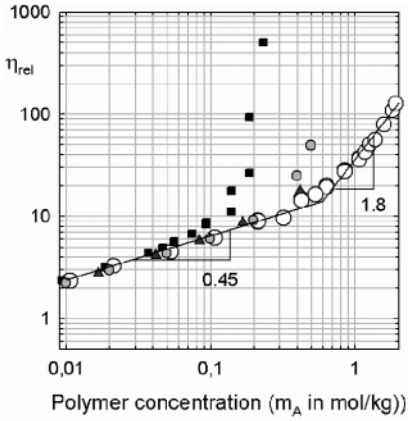

Figure 1. Comparison between relative viscosities of PAA derivatives in water at 25 °C: PAA (○), PAAg5C12 (●), PAAg10C12 (■), PAAgPNIPA (▲).

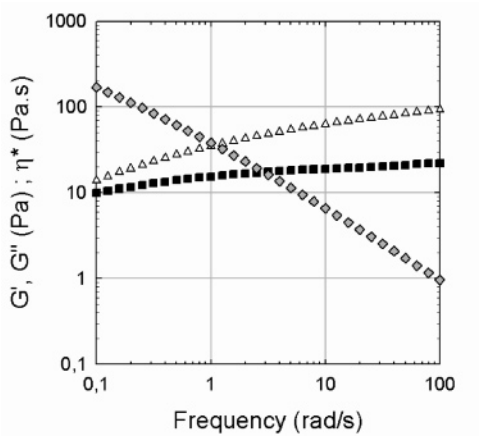

Figure 2. Viscoelastic properties of PAAg10C12 aqueous solution ($m_A = 0.36$ mol/kg, $T = 20$ °C): G' (△), G'' (■), η^* (◆).

pure D_2O sample, used as background, was subtracted from the scattering intensity of the copolymer sample. The efficiency of the detector cell was normalized by the intensity delivered by a pure water cell of 1 mm thickness. Absolute measurements of the scattering intensity $I(q)$ (cm^{-1} or 10^{-8} $Å^{-1}$) were obtained from the direct determination of the incident neutron beam flow and the cell solid angle.[29]

Results and Discussion

Regime of Concentration. Unlike nonionic macromolecular coils, polyelectrolyte rods start to overlap at extremely low concentration (C^*). Consequently, the semidilute regime spans over several decades of concentration, and the transition between dilute and semidilute regimes is often out of range of applications. If we first consider the viscosity of PAA solutions (Figure 1), a first regime is observed where the relative viscosity scales with the concentration at the power 0.45. This value is close to 1/2 as theoretically predicted[30] for both dilute and unentangled semidilute solutions. By increasing the concentration, a scaling transition was observed with a higher concentration dependence ($\alpha = 1.8$). Again this value is rather close to the one predicted for salt-free polyelectrolyte solutions in the semidilute entangled regime[30] ($\alpha = 3/2$).

For the PAA series, the entanglement concentration of polyelectrolyte chains (C_e) takes place around $m_A \sim 0.6$ mol/kg ($C_{PAA} \sim 5-6$ wt %). In the absence of association, the solutions of grafted PAA, like PAAgPNIPA, behave similarly to PAA, but as soon as associations take place, the behavior dramatically diverges, as observed with C12 derivatives for instance. Below 0.05 mol/kg, the viscosity of PAAg10C12 and PAA solutions are very close, and we can infer that in this concentration range and at low ionic strength the electrostatic repulsions overcome hydrophobic associations. However, the situation is effectively very different at higher ionic strength, when intramolecular hydrophobic associations take place. Above a critical aggregation concentration (cac), the viscosity of PAAg10C12 progressively departs from the polyelectrolyte behavior and then "diverges" with a high scaling exponent, taking into account the high conversion (intra → inter) of the hydrophobic aggregation.[14] At $m_A = 0.2$ mol/kg for example, the introduction of 1 dodecyl sticker every 10 acrylic acid units is responsible for a viscosity increase by 1 decade. By comparison, the cac of weak hydrophobically modified PAA, like PAAg5C12, is much higher, and the associating process is observed macroscopically only above 0.2 mol/kg.

For the following experiments, performed at $m_A = 0.3-0.6$ mol/kg, we consider that all the solutions are in the unentangled semidilute regime, just below the entanglement concentration.

Self-Assembling of Hydrophobically Modified PAA. The viscoelastic behavior of a PAAg10C12 solution at 0.36 mol/kg is given in Figure 2.

At this concentration hydrophobic side chains form efficient temporary cross-links between the polyelectrolyte chains, and the elastic behavior dominates on the whole frequency range studied. The first description of the transient network theory was given by Green and Tobolski[31] in 1946. According to their theory, the network is characterized by a single relaxation time (τ_N) and a high-frequency storage modulus which is given by

$$G_0 = \nu kT \tag{3}$$

where ν is the number concentration of elastically active chains, k is the Boltzmann constant, ant T is the absolute temperature. The theory predicts a constant steady-shear viscosity given by

$$\eta(\dot{\gamma}) = \eta_0 = G_0\tau_N = \nu kT\tau_N \tag{4}$$

In the past 15 years, several important theoretical works[12-15] have progressively given a more accurate description of the dynamic properties of physical networks taking into account either the structure of associating polymers (telechelic or multisticker), the type of association (pairwise or large aggregates), or the range of concentration for polymer chains (overlapped, entangled, etc.) The latter parameter is of prime importance, and according to the concentration regimes and subregimes, scaling relations are able to describe the concentration dependence of the modulus or the dynamic properties of the network: typically the characteristic time and the viscosity. However, one of the most important common features of these theories is that the terminal relaxation time of the network (τ_N) is proportional to the lifetime of the stickers in the aggregate (τ_b), as previously defined in eq 1. Clearly it means that the disengagement rate of the stickers from the micellar junction ($\beta = \tau_b^{-1}$) is the primary process controlling the flow properties of the physical network. Of course, if the lifetime becomes infinite or at least very

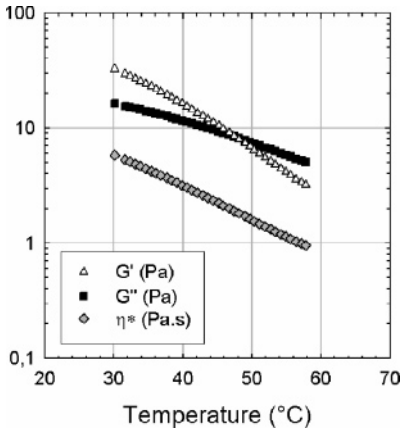

Figure 3. Viscoelastic properties of PAAg10C12 aqueous solution ($m_A = 0.36$ mol/kg; $\omega = 6.28$ rad/s): G' (△), G'' (■), η^* (◆).

long, as it is with chemical cross-links or vitreous-like aggregates, the dynamics no longer prevail in the common window of observation and the system behaves as a permanent network. In the case of physical gels, the temperature is the relevant parameter to probe the dynamic properties, and several ways can be followed to achieve such a treatment. The simplest method consists of following the complex viscosity, or the shear viscosity, with the temperature, and this can be carried out quite easily using rheometer equipped with a Peltier system with controlled temperature ramping facility. We show in Figure 3 the viscoelastic properties of PAAg10C12 measured as a function of temperature (heating rate of 2 °C/min) at $\omega = 6.28$ rad/s.

It can be readily seen that the variation of moduli G' and G'' cross each other at about 48 °C. This temperature can be used to define the gelation threshold, but this value is obviously frequency dependent.

For polymer solutions, Andrade's equation is generally applied to determine the activation energy of viscous flow (E_a):

$$\eta = B \exp\left(\frac{E_a}{kT}\right) \tag{5}$$

where B is a constant. In the case of associating polymer solutions, the activation energy can be closely compared to the potential barrier of the sticker (see relations 1 and 5), and we will discuss our data under this conjecture ($E_a \approx W$). In the conditions reported in Figure 3, we get $E_a = 55$ kJ/mol, but again this energy is a function of the frequency as the network is analyzed in the non-Newtonian regime. With similar extrapolations, $E_a = 36$ and 81 kJ/mol are obtained at frequencies of 100 and 0.1 rad/s, respectively. For comparison, the activation energy of a PAA solution is around 20 kJ/mol at the same concentration (0.36 mol/kg), in agreement with the activation energy of pure water ($E_a = 16$ kJ/mol). A more accurate determination of the activation energy of the solution can be done by applying a time−temperature superposition (TTS) of the moduli spectra obtained at different temperatures. In the case of PAAg10C12, we followed the same procedure as the one reported in Figure 2 by changing the temperature from 30 to 50 °C. From the simple model described in eqs 1, 3, and 4, it would be expected that dynamic mechanical moduli of an associating network can be superimposed

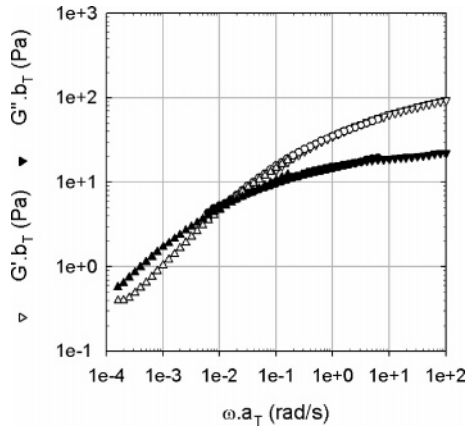

Figure 4. Time−temperature superposition of PAAg10C12 aqueous solution ($m_A = 0.36$ mol/kg; $T_{ref} = 20$ °C): G' (△, ○, ▽), G'' (▲, ●, ▼); (△) 50 °C, (○) 30 °C, (▽) 20 °C.

at any temperature T onto a single curve (T_{ref}) with the appropriate horizontal (a_T) and vertical (b_T) shift factors:

$$a_T = \frac{\beta(T_{ref})}{\beta(T)} = \exp\left\{-\frac{W}{kT}\left(\frac{1}{T_{ref}} - \frac{1}{T}\right)\right\} \tag{6}$$

and

$$b_T = \frac{kT_0\nu(T_{ref})}{kT\nu(T)} \tag{7}$$

The application of the TTS to PAAg10C12 solution is shown in Figure 4.

In this range of temperature, the vertical shift factor (b_T) accounting for the concentration of elastically active chains is nearly negligible. The horizontal shift factor (a_T) that directly correlates the frequency dependence with the temperature gives an activation enthalpy of 150 kJ/mol, much higher than those previously extrapolated at fixed frequency. Using the crossover frequency of moduli as an indication of the longest relaxation time of the network, the normalized frequency ($a_T\omega_c = 0.013$) gives characteristic times $\tau_c = 80$, 5, and 0.1 s at 20, 30, and 50 °C, respectively.

This result is in good agreement with TTS procedures performed on similar hydrophobically modified poly(sodium acrylate) by Petit,[32] but it strongly differs from other associating polymers like hydrophobically end-capped poly(ethylene glycol) (HEUR)[6] or grafted copolymers with a low modification content (<2 mol %), like HASE[9] or hydrophobically modified polyacrylamide.[11] For these systems, the activation energy is generally between 40 and 90 kJ/mol, depending on the primary structure and the nature of the alkyl group ($W \cong 42$ kJ/mol in the case of HEUR end-capped with C12).[9] The difference observed between these systems and PAAg10C12 could be due to the higher extent of hydrophobic modification of the polymer chain (10 mol % in the present case). In the theoretical descriptions of associating polymers, the number of solvophilic monomers between two stickers is generally assumed to be very large, and then the elementary step of the sticky Rouse motion is simply related to the single transfer of one sticker from a micellar junction to another. In the case of PAAg10C12, the average number of sodium acrylate units between two stickers is small (~9), and the random nature of the grafting cannot avoid the existence of closer stickers, even twinned,

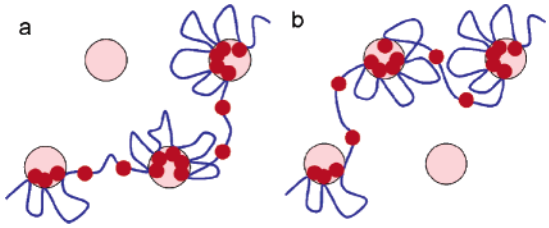

Figure 5. Schematic description for self-assembling of PAAg10C12 in aqueous solution. Hopping of a chain from one micellar junction (a) to another one (b) involves a simultaneous disengagement of several stickers. (for clarity, other chains and stickers are not shown).

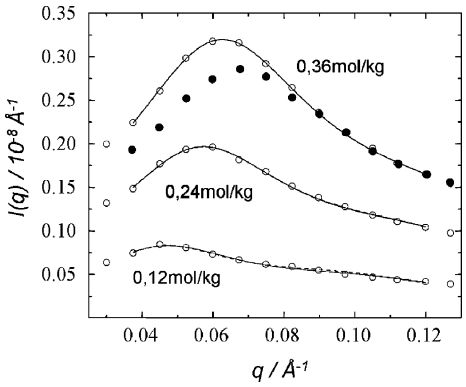

Figure 6. Scattering profiles of PAAg10C12/D_2O solutions at different concentrations: (○) experimental data and (—) model fitting at 20 °C; (●) experimental data at 60 °C.

which can dramatically modify the dynamics of the polymer chain. Another important consequence that we will discuss in the foregoing, is that the average distance between aggregates could be much larger than the average distance between two topological alkyl neighbors. The main consequences are (1) a broad distribution of the relaxation times with a strong departure from the single element Maxwell model where fast modes superimpose to slow relaxation process and (2) an increase of the activation energy as the disengagement rate of n stickers at the same time is now controlling the sticky Rouse dynamics of the polymer chain (see Figure 5).

To correlate the macroscopic properties to the structure of the physical network, SANS experiments were performed with PAAg10C12 solutions in D_2O. The scattering intensities are shown in Figure 6 for three different polymer concentrations and two temperatures used for the highest concentration (0.36 mol/kg). All the scattering curves display the signature of an organized structure with a correlation peak at q_{max} that shifts toward higher q values (or smaller distances) with increasing concentration. Taking the maximum of this peak (q_{max}) as an indication of the average distance between hydrophobic aggregates ($d = 2\pi/q_{max}$), we get a scaling relation between the distance and the concentration with an exponent close to 1/3, as expected for a typical dilution law. At the same time we observe a small decrease of the peak intensity by increasing the temperature in correlation with the Arrhenius behavior of the association process ($W > 0$).

A deeper analysis of these scattering curves can be carried out by using a simple micellar model. Generally used to describe block copolymers forming micellar structures, such model has been successfully applied recently to graft copolymers.[33] In the micellar model, we consider spherical polydisperse micelles of C12 with

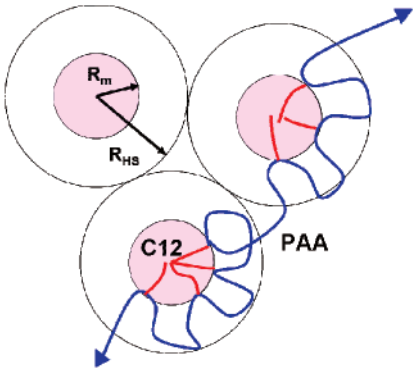

Figure 7. Schematic description of the micellar model with hard-sphere interactions used to describe self-assembling of grafted PAA.

an average radius R_m and a Gaussian size distribution of their size $\omega(r)$, embedded in a sea of PAANa chains that make bridges and loops around the cores (Figure 7). In that case, the form factor is given by

$$F(q) = \int_{R_1-5\sigma}^{R_1+5\sigma} f(q,r)\,\omega(r)\,\mathrm{d}r \tag{8}$$

where $f(q,r)$ is the form factor of a sphere of radius r given by (9) and $\omega(r)$ is the Gaussian size distribution given by (10) with R_m the average radius and σ the standard deviation:

$$f(q,r) = \left[4\pi r^3 \frac{\sin(qr) - qr\cos(qr)}{(qr)^3}\right]^2 \tag{9}$$

The Gaussian distribution is given by

$$\omega(r) = \frac{1}{\sqrt{2\pi}\sigma}\exp\left(-\frac{(r-R_m)^2}{2\sigma^2}\right) \tag{10}$$

In this model, all C12 grafts do not participate to the micelles, and the fraction of grafts in micelles, f_{C12}, is used as a fitting parameter.

Knowing the core radius R_m, the number of grafts per aggregate N_{ag} can be determined (11) and then the number of micelles per volume unit, $[N_m]$ (12):

$$N_{ag} = \frac{\frac{4}{3}\pi {R_m}^3}{v_{C12}} \tag{11}$$

$$[N_m] = \frac{f_{C12} C_p \tau_{C12} N_A}{M_{C12} N_{ag}} \tag{12}$$

where v_{C12} is the molecular volume of dodecyl chain, C_p is the copolymer concentration, τ_{C12} is the weight fraction of C12 in the copolymer, M_{C12} is the molar mass of C12, and N_A is the Avogadro number.

In this model, the micelles are assumed to repulse each other with a hard-sphere potential (Figure 7), and the Percus−Yevick approach is considered. The structure factor for hard spheres of radius R_{HS} can be expressed as

$$S(q) = \left[1 + \frac{24\phi_{HS} G(2qR_{HS})}{2qR_{HS}}\right]^{-1} \tag{13}$$

where $G(2qR_{HS})$ is a trigonometric function[33] depending on q, R_{HS}, and ϕ_{HS}.

Table 2. Fitting Parameters Obtained from SANS Performed on PAAg10C12/D_2O Solutions at $T = 20°C$ ($\phi_m = 1$, N_A = Avogadro's Number)

m_A (mol/kg)	q_{max} (Å^{-1})	f_{C12}	R_m (Å)	σ (Å)	R_{HS} (Å)	ϕ_{HS}	$[N_m]/N_A$ (mol/m^3)	N_{ag}
0.12	0.045	0.62	13.9	2.9	59.3	0.10	0.19	36
0.24	0.060	0.70	14.7	1.7	48	0.11	0.39	41
0.36	0.064	0.75	15.2	1.5	43.5	0.12	0.58	45

ϕ_{HS} is the volume fraction of hard spheres determined according to eq 14:

$$\phi_{HS} = \left(\frac{4}{3}\pi {R_{HS}}^3\right)[N_m] \quad (14)$$

Finally, SANS scattering intensity ($I(q)$) for particles immersed in a continuous medium can be expressed by the following equation, where $\Delta\rho$ is the contrast of scattering length density:

$$I(q) = [N_m](\Delta\rho)^2 F(q)\, S(q) \quad (15)$$

This model, based on a simple description of the form factor (spherical objects) and the structure factor (hard-sphere repulsions), was applied to our results using an absolute fitting of the data. It gives an unequivocal set of parameters: f_{C12}, R_m, σ, R_{HS}, and ϕ_m which allow the calculation of the hard-sphere fraction (ϕ_{HS}), the micelle concentration [N_m], and the aggregation number (N_{ag}). An example is given in Figure 6, and the main results of these fittings are summarized in Table 2.

Following the hard-sphere concentration ([N_m]), we verify that the number of micelles is proportional to the polymer concentration. Once again, the validity of the dilution law can be correlated to the existence of scattering centers (micelles) that do not change substantially with the concentration (ϕ_m, R_m, and N_{ag}). Other interesting aspects can be underlined from this fitting: (1) The volume fraction of C12 inside the core is close to 1 as expected for highly hydrophobic micelles. (2) The average radius of the cores, of about 15 Å, fits nicely with the geometric distance calculated between the first and the end carbon of the C12 side chain in a zigzag planar conformation (~14 Å). (3) The aggregation number is also in good agreement with similar hydrophobic clusters like SDS micelles ($N_{ag} = 60$) or C12 cores obtained from PAAgC12 self-assembling. Applying various techniques like X-ray scattering, ^{13}C NMR, and time-resolved fluorescence, Petit[32] found aggregation numbers for C12 side chains ranging between 40 and 60.

Another interesting parameter is f_{C12}, the fraction of aggregated side chains, and similar information can also be obtained from ^{13}C NMR. This has been well described in the case of PAA grafted with alkyl or perfluoroalkyl side chains by Petit et al.[34] In their work, they use the fact that the chemical shifts of hydrophobic carbons, which belong to aliphatic side chains, depend on the chemical environment. This environment changes appreciably whether the hydrophobic tail is free in aqueous solution (polar aqueous environment) or aggregated within micelles (low-polarity environment). If the exchange is slow, with respect to the NMR characteristic time scale, a clear peak splitting is observed corresponding to free and aggregated forms at high and low fields, respectively. The ^{13}C NMR spectrum of a PAAg10C12 aqueous solution ($m_A = 0.36$ mol/kg) is given in Figure 8. From there we can easily observe the peak splitting corresponding to terminal methyl group ($\delta \sim 14$ ppm) and vicinal methylene carbon ($\delta \sim 22$ ppm). By integrating the different signals corresponding to free and aggregated hydrophobic tails, using either $\mathbf{CH_2}CH_3$ or $\mathbf{CH_3}$ groups, it follows that about 2/3 of C12 are aggregated which is in rather good agreement with SANS fitting ($f_{C12} = 0.74$ at the same concentration).

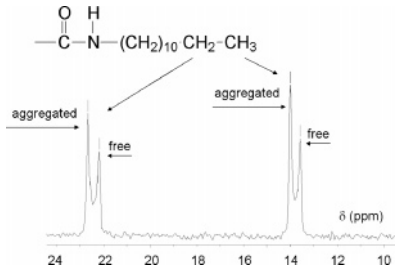

Figure 8. ^{13}C NMR spectrum of PAAg10C12 solution in D_2O (0.36 mol/kg). Peak splitting observed for terminal methyl group (~14 ppm) and vicinal methylene carbon (~22 ppm) correspond to free and aggregated form, at high field and low field, respectively.

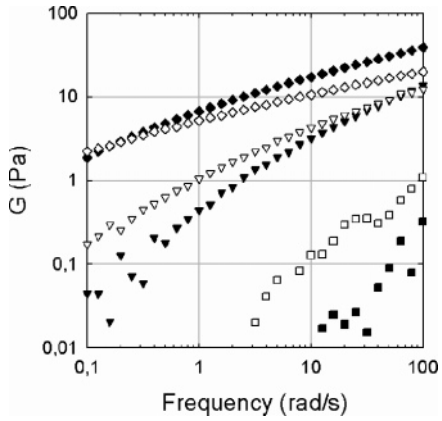

Figure 9. Dynamic moduli of PAAgPNIPA aqueous solution ($m_A = 0.42$ mol/kg) at different temperatures: □, 30 °C; ▽, 50 °C; ◇, 60 °C. G' (filled symbols) and G'' (open symbols).

The final picture that can be proposed for PAAg10C12 solutions is that for concentrations between 0.1 and 0.4 mol/kg self-assembly is very far from the crystal organization found with poloxamers at high concentration and/or high temperature. Nevertheless, the system self-organized around micellar aggregates interconnected through PAA backbones. According to this model, the average distance between hydrophobic cores ($d = 2(R_{HS} - R_m)$) decreases smoothly with the concentration but still remains higher ($d = 57$ Å for $m = 0.36$ mol/kg) than the average sequence length between two stickers ($l = 25$ Å, assuming a complete extension of the chain). Consequently, the fraction of intramolecular associations remains high at these polymer concentrations, and this strongly influences the dynamics of the associating network (see Figure 5).

Self-Assembling of LCST Modified PAA. The dynamic moduli of PAAgPNIPA aqueous solutions are reported in Figure 9.

At low temperatures, solutions of PAAgPNIPA are liquidlike, as PAA solutions. Above 30 °C, physical gelation occurs and at 60 °C, the solution displays a

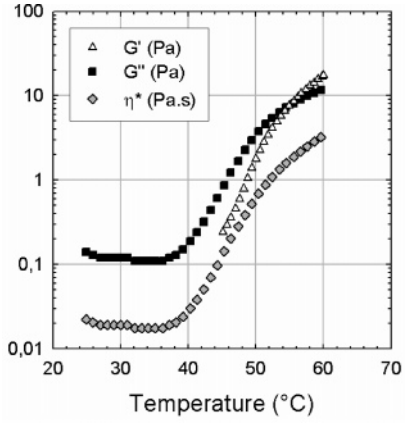

Figure 10. Viscoelastic properties of PAAgPNIPA aqueous solution ($m_A = 0.42$ mol/kg; $\omega = 6.28$ rad/s): G' (△), G'' (■), η^* (◆).

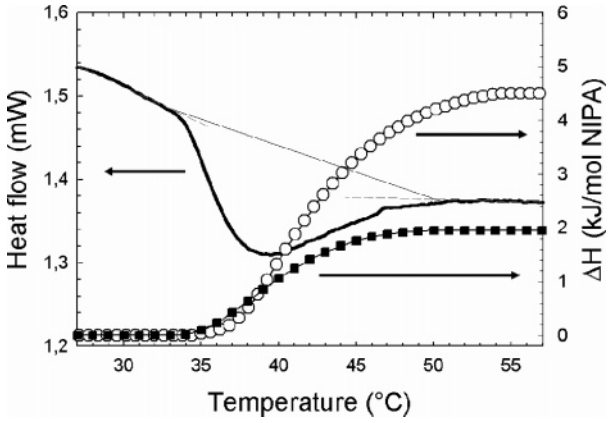

Figure 11. Heat flow (solid line) and transition enthalpy (■) of an aqueous solution of PAAgPNIPA ($m_A = 0.42$ mol/kg). Transition enthalpy of PNIPA precursor in similar conditions ($C_{PNIPA} = 1$ wt %, ○). Heating rate = 1 °C/min.

strong elastic behavior as previously reported with PAAg10C12 at low temperature. The sol/gel transition and the thermothickening behavior of PAAgPNIPA in aqueous solution are more easily demonstrated by ramping the temperature at constant frequency. As shown in Figure 10, the polymer solution is characterized by an initial decrease of viscosity in the low-temperature range ($E_a = 20$ kJ/mol as for PAA solution at the same concentration) followed by a strong thickening induced by the local microscopic phase separation of PNIPA side chains at about 35 °C. In the experimental conditions ($\omega = 6.28$ rad/s) a crossover between G' and G'' is obtained around 55 °C.

The association process of PNIPA can be followed by other techniques such as ^{1}H or ^{13}C NMR spectroscopy (formation of vitreous aggregates) or DSC (endothermic phase transition). The thermogram of an aqueous solution of PAAgPNIPA is reproduced in Figure 11 with its transition enthalpy. The endotherm related to the coil ⇒ globule transition is ranging between 34 and 50 °C, with a corresponding heat change of $\Delta H \cong 2.0$ kJ/(mol NIPA). Under similar conditions, PNIPA precursor undergoes a sharper transition ($\Delta H = 4.5$ kJ/mol) starting at similar temperature (34 °C). These differences (Figure 11) can be ascribed to the strong electrostatic repulsions that take place between polyelectrolyte backbones, which prevents the phase separation process of LCST side chains. By comparing the enthalpy values we can assume that the dehydration process of the PNIPA grafts is not quantitative and about half of the NIPA units remain hydrated even at high temperature. There appears to be a strong correlation between the dehydration process observed by DSC and the thermogelation induced at the macroscopic level.

Obviously, the LCST type phase separation of PNIPA side chains is the driving force of the network formation, but another important feature is that even after the process of self-assembling (above 50 °C), the viscosity tends to increase with increase in temperature, following an Arrhenius behavior with a "negative activation energy". Unfortunately, the TTS procedure cannot be applied easily to PAAgPNIPA solutions, mainly because the PNIPA side chains form vitreous aggregates[35] that considerably slow down the dynamics of the physical network. Nevertheless, by shifting the isotherms obtained at high temperature (above T_{ass}) along the x-axis, it is possible to estimate the activation energy of PAAgPNIPA solution between −300 and −500 kJ/mol in the strong segregation regime.

To understand the opposite behaviors found between associating polymers bearing either PNIPA or C12 side chains, we can draw a parallel between the enthalpy of demicellization of surfactants and the activation energy of the same stickers, which leave temporarily the micellar junction. This process is clearly exothermic for PNIPA (as observed from DSC); meanwhile, the question remains open for hydrophobic molecules. Here, one can draw an anology from the dissolution of hydrocarbons in water, which involves two main processes:[36] (1) breaking of van der Waals interactions between hydrocarbons molecules ($\Delta H_{vdW} > 0$); (2) modification of hydrogen bonding in solutions resulting from the hydration of hydrocarbon molecules ($\Delta H_{hyd} < 0$).

Concerning the dissolution of hydrocarbons in water, the overall enthalpy of mixing (ΔH_{mix}) is a balance between the two opposite contributions, and its sign varies with the chain length. At 25 °C, a linear relation is obtained between ΔH_{mix} of low hydrocarbons and their number of carbons (n):

$$\Delta H_{mix} = -15 + 2.6n \quad \text{(kJ/mol)} \tag{16}$$

This relation describes that the mixing of hydrocarbons in water becomes less favorable with increasing the chain length. The enthalpy is exothermic for low hydrocarbons up to pentane, athermic for hexane, and endothermic for higher alkanes. Moreover, the enthalpy of demicellization ($\Delta H_{demic} \cong \Delta H_{mix}$) could be temperature dependent. In the case of SDS in water, the enthalpy shows a linear relationship with temperature: ΔH is negative at low temperature (below 25 °C) and becomes positive above this value.[37] If we assume, that like SDS, ΔH_{demic} is endothermic for C12 side chains in the high-temperature range, eq 1 tells us that the lifetime of dodecyl groups and the characteristic time of the network will decrease with increasing temperature ($W > 0$) while PNIPA derivatives will behave oppositely ($W < 0$).

As reported for PAAg10C12 in the previous section, the association process of thermothickening polymers can also be studied by SANS. In that case, the transition occurring above 30 °C is clearly evidenced by the growth of a strong scattering peak around $q_{max} \sim 0.015$ Å^{-1} (Figure 12). Compared to PAAg10C12, the lower values of q_{max} are correlated with larger distances between the aggregates. By applying the same model as before (polydisperse spherical micelles with hard sphere in-

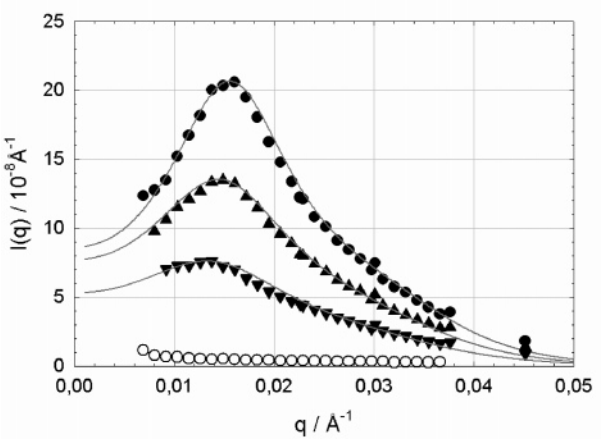

Figure 12. Scattering profiles of PAAgPNIPA/D_2O solutions at different concentrations (●, 0.56 mol/kg; ▲, 0.42 mol/kg; ▼, 0.28 mol/kg) experimental data and (—) model fitting at 60 °C (○, 0.56 mol/kg) experimental data at 20 °C.

teractions), we get the set of data reported in Table 3. At high temperature, PNIPA self-assemble into large aggregates which remain roughly independent of polymer concentration.

The micelle concentration ($[N_m]$) is again proportional to the polymer concentration as expected for dilution law. The core radius of PNIPA aggregates is quite large ($R_m \sim 77$ Å) compared to the radius of C12 micelles, but this is expected as PNIPA side chains are much longer than dodecyl groups. Assuming a Gaussian coil conformation of PNIPA chains, its end-to-end distance is found close to 50 Å. This result is consistent with the radius of the core ($R_m \sim 77$ Å), assuming some extension of PNIPA chains. The fraction of PNIPA inside the core is estimated between 0.6 and 0.7. Considering the glass transition temperature of pure PNIPA ($T_g \cong 135$ °C), these high volume fractions are in good agreement with the vitreous-like character of aggregates.[35]

The results of the fitting also point out that only 50−60% of PNIPA side chains participate in the formation of the aggregates. This value is still in rather good agreement with the fraction of dehydrated PNIPA obtained from DSC (∼45% for a concentration of 0.42 mol/kg) or with the fraction of frozen PNIPA that can be obtained in similar conditions from ^1H NMR experiments.[38] Finally, on the basis of the schematic description given in Figure 5, the average distance between PNIPA cores is equal to $d = 200$ Å, i.e., equal to or smaller than the distance between two vicinal side chains ($l = 600$ Å on the basis of a zigzag conformation). By comparison with PAAg10C12 solutions, where the average distance between hydrophobic aggregates was always higher than the mean distance between neighboring stickers, we expect a higher bridge/loop ratio for low grafted copolymers such as PAAgPNIPA.

We have seen that PAAgC12 and PAAgPNIPA are characterized by opposite thermal properties in aqueous solution, and the next section of this paper deals with the structure and the properties of mixtures of these polymers in aqueous solutions.

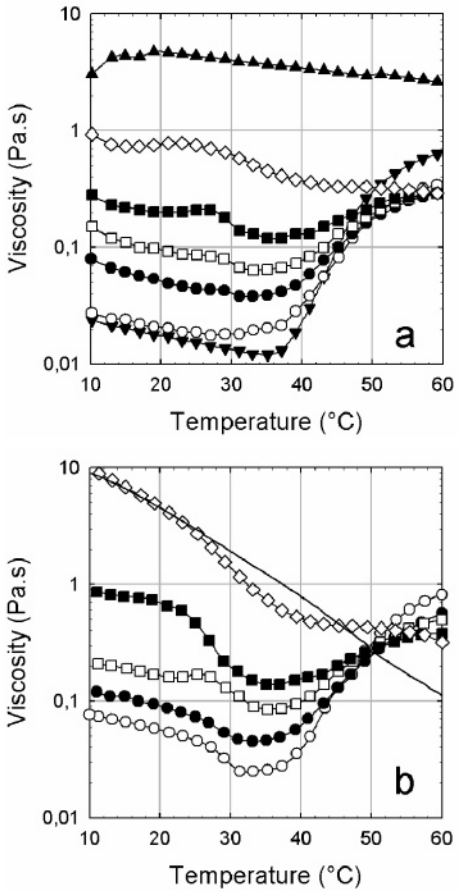

Figure 13. Viscosity of aqueous mixtures of PAAgPNIPA + PAAg10C12 for different compositions [$m_{PAAgPNIPA}/m_{PAAg10C12}$]. Total concentration: $m_A = 0.42$ mol/kg. (a) Shear viscosity ($\gamma = 100$ s^{-1}); (b) complex viscosity ($\omega = 6.28$ rad/s): ▼, [0.42/0]; ○, [0.34/0.08]; ●, [0.25/0.17]; □, [0.21/0.21]; ■, [0.17/0.25]; ◇, [0.08/0.34]; ▲, [0/0.42]. The reference line in (b) corresponds to PAAg10C12; $m_A = 0.32$ mol/kg.

Mixtures of Thermothinning and Thermothickening Copolymers. The first series of mixtures were prepared by keeping constant the overall polymer concentration, $m_A = 0.42$ mol/kg, while changing the relative proportion of each copolymer. In Figure 13a we report the steady-shear viscosity as a function of temperature at $\gamma = 100$ s^{-1}.

A first analysis of these curves indicates that intermediate viscoelastic properties can be readily obtained by mixing PAAgPNIPA and PAAg10C12. At low temperature, PNIPA side chains do not aggregate, and the behavior is very similar to what we can expect from a simple mixture PAAg10C12 + PAA. The transition temperature of PNIPA does not change with the added PAAg10C12 ($T_{ass} \approx 34$ °C), and this was also confirmed by DSC. At high temperature, both C12 and PNIPA self-associate, but the viscosity of the mixtures is always smaller than that of the pure samples. A very similar behavior has been reported by Jimenez Regalado et al.[39] with unentangled mixtures of two hydrophobically modified polyacrylamide (HMPAM) with very different

Table 3. Fitting Parameters Obtained from SANS Performed on PAAgPNIPA Aqueous Solutions at $T = 60$ °C (N_A = Avogadro's Number)

m_A (mol/kg)	q_{max} (Å^{-1})	f_{NIPA}	R_m (Å)	σ (Å)	ϕ_m	R_{HS} (Å)	ϕ_{HS}	$[N_m]/N_A$ (mol/m^3)	N_{ag}
0.28	0.0137	0.50	76	10	0.60	178	0.07	5.2×10^{-3}	117
0.42	0.0149	0.55	77	10	0.65	174	0.10	7.5×10^{-3}	132
0.56	0.016	0.62	77	10	0.68	172	0.14	10.9×10^{-3}	138

hydrophobic characteristics. It was interpreted in terms of weak segregation between polymers or microphase separation. Under similar conditions, mixtures of HM-PAM and PAM lead to phase separation above a critical polymer concentration. This phase separation process in mixtures of associating polymers has also been described theoretically and experimentally by Annable et al.[40] with poly(ethylene oxide) end-capped at both ends by alkyl groups. Considering the effect of association of end groups within the Flory−Huggins scheme, they proposed a model based on the gain of entropy due to the associations between the hydrophobic units.

Obviously in our mixtures, there is no specific interaction between PNIPA and C12 as it was reported with similar systems like PNIPA + SDS[41] or PAAgC18 + long PNIPA chains.[42] In the present case, this can be explained by the small size of PNIPA chains and the strong repulsive interactions between polyelectrolyte backbones. From the viscosity profiles in Figure 13a one can see some overshoot at a temperature close to 25 °C, but under these conditions, the high shear rate levels off the viscosity behavior. When the same experiments are reproduced at low deformation (Figure 13b, $\omega = 6.28$ rad/s), some transition can be readily observed in the course of viscosity vs temperature: (1) below 20−25 °C the viscosity decreases smoothly with the temperature; (2) above 25 °C the viscosity starts to decrease more rapidly until the transition temperature of PNIPA around 34 °C. As in the case described by Jimenez Regalado et al.,[39] this transition points out the microphase separation taking place between polymers, and the fact that this transition occurs upon heating is in good agreement with the theoretical predictions of Annable et al.[40] This small transition is also easily evidenced in Figure 13b by the comparison between the viscosity of PAAg10C12 alone (m = 0.32 mol/kg) and "PAAg10C12 (m = 0.34 mol/kg) + PAAgPNIPA (m = 0.08 mol/kg)". In that case we can see that at low temperature (below 23 °C) the viscosity is mainly controlled by the associating properties of the copolymer PAAg10C12. However, above 23 °C the mixture viscosity starts to drop rapidly as a result of the microscopic phase separation. Then, when the temperature reaches the transition of PNIPA, the formation of the second network stiffens the properties of the physical gel, and at high temperature, the viscosity of the mixture becomes higher than that of the solution of PAAg10C12.

Another comparison between a copolymer mixture and a pure copolymer solution is given in Figure 14 where the viscoelastic properties have been plotted at either constant temperature (T = 40 °C) or constant frequency ($\omega = 6.28$ rad/s).

At 40 °C, the addition of PAAg10C12 dramatically increases the viscoelastic properties of PAAgPNIPA. The solution becomes highly viscous by 2 orders of magnitude in viscosity. The properties are enhanced in the whole range of temperatures (Figure 14b), and mixtures appear as a reasonable way to control the rheology of formulations toward environmental conditions. Indeed, this combination gives rise to high viscosity at low temperature and thermothickening properties. Nevertheless, the stability with time of such "microphase-separated networks" will depend on both temperature and viscosity. For example, mixtures of PAAgPNIPA + PAAg10C12 will macroscopically phase separate if the solution is stored for several months at room temperature.

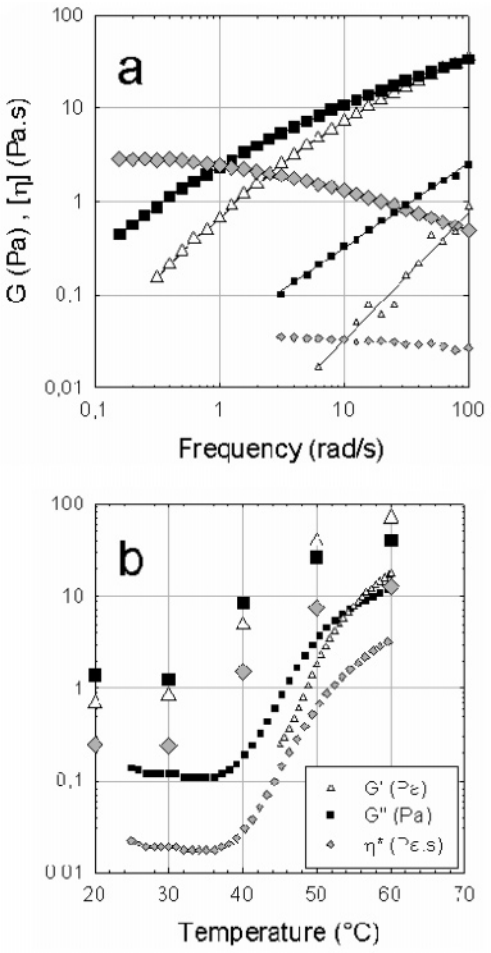

Figure 14. Viscoelastic properties of aqueous solution of PAAgPNIPA (m = 0.42 mol/kg): small symbols and mixture of "PAAgPNIPA (m = 0.42 mol/kg) + PAAg10C12 (m_A = 0.24 mol/kg)": large symbols. G' (△), G'' (■), η^* (◆). (a) T = 40 °C, (b) ω = 6.28 rad/s.

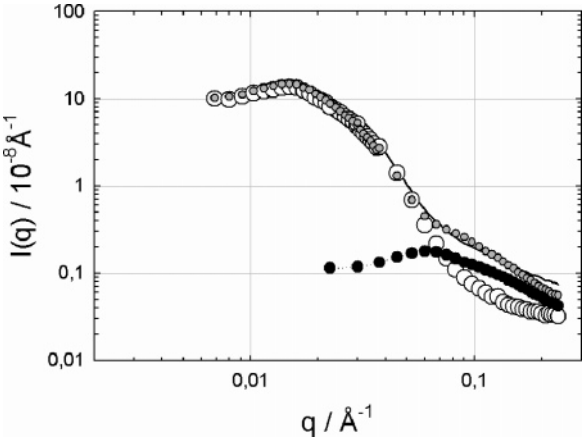

Figure 15. Scattering profiles of copolymer solutions in D_2O (T = 60 °C): I_1 = ○: PAAgPNIPA (0.42 mol/kg); I_2 = ●: PAAg10C12 (0.24 mol/kg); I_3 = •: "PAAgPNIPA (0.42 mol/kg) + PAAg10C12 (0.24 mol/kg)"; —: calculated curve corresponding to $I_4 = I_1 + I_2$ at 60 °C.

A deeper analysis of the structure corresponding to the mixture of associating copolymers has been done by SANS. In Figure 15, we compare the scattering patterns of copolymer solutions (D_2O, T = 60 °C) of PAAgPNIPA (0,42 mol/kg), PAAg10C12 (0.24 mol/kg), and "PAAgPNIPA (0.42 mol/kg) + PAAg10C12 (0.24 mol/kg)".

As previously described, the scattering peaks originating from each copolymer solutions are easily distinguished as they are situated in very different q range (different local structure). The intriguing result is that the experimental data obtained with the mixture of copolymers can be fitted using the additive contributions of the original scattering signals obtained with each polymer solutions. This means the correlations between PNIPA aggregates are not modified by the presence of PAAg10C12, and the same holds for C12 micelles. Clearly, the copolymers do not self-assemble with an interpenetrated structure but form some composite architecture which confirms the previous picture of "microphase-separated networks".

Conclusion

The results reported in this paper show that thermal properties of water-soluble associating polymers result from a subtle balance taking into account (1) van der Waals interactions between hydrophobic moieties, (2) hydrogen bonds between water molecules, and (3) hydration of hydrophobic groups (modification of hydrogen bonding). Depending on the nature of the stickers, either thermothinning or thermothickening behaviors can be obtained. This is demonstrated with poly(sodium acrylate) modified either by hydrophobes (alkyl chains) or responsive polymers like PNIPA. At any temperature, the dynamics of the associating network is strongly correlated to the lifetime of the stickers through their enthalpy of demicellization. In the unentangled semidilute regime, polymer networks display surprisingly high activation energy (positive or negative) that takes into account the high grafting ratio of PAAg10C12 or the low mobility of PNIPA in vitreous-like aggregates. The structural characteristics of these networks are in close relation with the primary structure of the copolymers, and the same SANS model is able to describe the different self-assemblies. Finally, we point out the mixtures of associating polymers, which could be used to control the rheology of aqueous fluids in a given environment. As described with nonionic systems, the mixtures of associating polyelectrolyte also exhibit phase segregation, and this transition is induced by heating. Nevertheless, at high temperature, the microphase-separated network remains stable with time certainly because the relaxation process is very long. The resulting viscoelastic properties are intermediate between both the individual copolymer solutions, but the segregation has a tendency to weaken the elastic behavior. From a fundamental point of view, this segregation process between associating polymers is an important problem for the technological applications, and the initial aim of the work which was to consider mixtures of polymers bearing antagonistic stickers has to be reconsidered in the light of these results. Following the same goal, several directions can be followed to minimize the segregation of associating networks. One possibility is to consider the introduction of antagonistic stickers in the same polymeric backbone (double-grafted copolymers) while the other possibility is to develop specific attractions between heterostickers belonging to different chains. These approaches will be reported in forthcoming papers.

Acknowledgment. Financial support for this project by IFCPAR, New Delhi, is gratefully acknowledged.

References and Notes

(1) *Water-Soluble Polymers, Synthesis, Solution Properties and Applications*; Shalaby, S. W., McCormick, C. L., Butler, G. G., Eds.; ACS Symposium Series 467; American Chemical Society: Washington, DC, 1991.
(2) Iliopoulos, I.; Wang, T. K.; Audebert, R. *Langmuir* **1991**, *7*, 617.
(3) Hill, A.; Candau, F.; Selb, J. *Prog. Colloid Polym. Sci.* **1991**, *84*, 61.
(4) Annable, T.; Buscall, R.; Ettelaie, R.; Whittlestone, D. J. *J. Rheol.* **1993**, *37*, 695.
(5) Yekta, B. Xu.; Duhamel, J.; Adiwidjaja, H.; Winnik, M. A. *Macromolecules* **1995**, *28*, 956.
(6) Annable, T.; Buscall, R.; Ettelaie, R.; Whittlestone, D. *J. Rheol.* **1993**, *37(4)*, 695.
(7) Petit, F.; Iliopoulos, I.; Audebert, R.; Szonyi, S. *Langmuir* **1997**, *13,* 4229.
(8) Cathebras, N.; Collet, A.; Viguier, M.; Berret, J.-F. *Macromolecules* **1998**, *31,* 1305.
(9) Tam, K. C.; Farmer, M. L.; Jenkins, R. D.; Basset, D. R. *J. Polym. Sci., Part B: Polym. Phys.* **1998**, *36*, 2275.
(10) Regalado, E. J.; Selb, J.; Candau, F. *Macromolecules* **1999**, *32*, 8580.
(11) Caputo, M. R.; Selb, J.; Candau, F. *Polymer* **2004**, *45*, 321.
(12) Leibler, L.; Rubinstein, M.; Colby, R. H. *Macromolecules* **1991**, *24*, 4701.
(13) Tanaka, F.; Edwards, S. F. *J. Non-Newtonian Fluid Mech.* **1992**, *43*, 247.
(14) Rubinstein, M.; Semenov, A. N. *Macromolecules* **2001**, *34*, 1058.
(15) Semenov, A. N.; Rubinstein, M. *Macromolecules* **2002**, *35*, 4821.
(16) Heymann, E. *Trans. Faraday Soc.* **1935**, *31*, 846.
(17) Suzuki, K.; Taniguchi, Y.; Enomoto, T. *Bull. Chem. Soc. Jpn.* **1972**, *45*, 336.
(18) Desbrieres, J.; Hirrien, M.; Rinaudo, M. *Carbohydr. Polym.* **1998**, *37*, 145.
(19) Carlsson, A.; Karlstrom, G.; Lindman, B. *Colloids Surf.* **1990**, *47*, 147.
(20) Brown, W.; Schillen, K.; Hvidt, S. *J. Phys. Chem.* **1992**, *96*, 6038.
(21) Mortensen, K.; Brown, W.; Jorgensen, E. *Macromolecules* **1994**, *27*, 5654.
(22) Hourdet, D.; L'Alloret, F.; Audebert, R. *Polymer* **1994**, *35*, 2624.
(23) Hourdet, D.; L'Alloret, F.; Audebert, R. *Polymer* **1997**, *38*, 2535.
(24) Hourdet, D.; L'Alloret, F.; Durand, A.; Lafuma, F.; Audebert, R.; Cotton, J. P. *Macromolecules* **1998**, *31*, 5323.
(25) Bromberg, L. *Macromolecules* **1998**, *31*, 6148.
(26) Durand, A.; Hervé, M.; Hourdet, D. In *Stimuli-Responsive Water Soluble and Amphiphilic Polymers;* McCormick, C. L., Ed.; ACS Symposium Series 780; American Chemical Society: Washington, DC, 2000; Chapter 11, p 181.
(27) Bokias, G.; Mylonas, Y.; Staikos, G.; Bumbu, G. G.; Vasile, C. *Macromolecules* **2001**, *34*, 4958.
(28) Durand, A.; Hourdet, D. *Polymer* **1999**, *40*, 4941.
(29) Cotton, J. P. In *Neutron, X-ray and Light Scattering*; Lindner, P., Zemb, T., Eds.; Elsevier: North-Holland, 1991; p 1.
(30) Dobrynin, A. V.; Colby, R. H.; Rubinstein, M. *Macromolecules* **1995**, *28*, 1859.
(31) Green, M. S.; Tobolski, A. V. *J. Chem. Phys.* **1946**, *14*, 80.
(32) Petit, F. Ph.D. Dissertation, University of Paris 6, 1996.
(33) Barbier, V.; Hervé, M.; Sudor, J.; Brulet, A.; Hourdet, D.; Viovy, J. L. *Macromolecules* **2004**, *37*, 5682.
(34) Petit-Agnely, F.; Iliopoulos, I. *J. Phys. Chem. B* **1999**, *103*, 4803.
(35) Afroze, F.; Nies, E.; Berghmans, H. *J. Mol. Struct.* **2000**, *554*, 55.
(36) Lichtenberg, D.; Opatowski, E.; Kozlov, M. M. *Surf. Sci. Ser.* **2001**, *93*, 295.
(37) Paula, S.; Süs, W.; Tuchtenhagen, J.; Blume, A. *J. Phys. Chem.* **1995**, *99*, 11742.
(38) Durand, A.; Hourdet, D.; Lafuma, F. *J. Phys. Chem. B* **2000**, *104*, 9371.
(39) Jimenez Regalado, E.; Selb, J.; Candau, F. *Macromolecules* **2000**, *33*, 8720.
(40) Annable, T.; Ettelaie, R. *Macromolecules* **1994**, *27*, 5616.
(41) Lee, T.-T.; Cabane, B. *Macromolecules* **1997**, *30*, 6559.
(42) Bokias, G.; Hourdet, D.; Iliopoulos, I.; Staikos, G.; Audebert, R. *Macromolecules* **1997**, *30*, 8293.

MA050786R